Bulgarian Chemical Communications, Volume 58, Issue 2 (pp. 154-161) 2026 *DOI: 10.34049/bcc.58.2.5735*

$NiFe_2O_4$@Cellulose-PEG nanocomposite: A novel reusable catalyst for straightforward one-pot synthesis of benzopyran derivatives

S. M. Awari[1], V. V. Vikhe[1], V. K. Vikhe[2], A. G. Gadhave[1], B. K. Uphade[1]*

[1]*Department of Chemistry and Research Centre, Padmashri Vikhe Patil College of Arts, Science & Commerce, Pravaranagar, (Affiliated to Savitribai Phule Pune University, Pune),413713, Dist: Ahilyanagar, Maharashtra, India*
[2]*Sir Visvesvaraya Institute of Technology, Chincholi, Tal: Sinnar Dist: Nashik, 422101. Maharashtra, India*

Received: December 09, 2025; Revised: March 26, 2026

This work presents the effective synthesis, characterization, and catalytic application of a novel $NiFe_2O_4$@Cellulose-PEG nanocomposite. The latter was synthesized by a simple co-precipitation method, and FT-IR, XRD, EDX, and SEM analysis techniques were used to characterize it. As an effective and affordable nanocatalyst, $NiFe_2O_4$@Cellulose-PEG effectively assisted the production of benzopyran derivatives by one-pot condensation of aromatic aldehydes, dimedone, and malononitrile. The yield of benzopyran was determined utilizing a number of reaction parameters, including catalyst quantity, solvent type, temperature, and reaction duration. By using ^{1}H NMR, ^{13}C NMR and MS studies, some of the synthesized benzopyran derivatives were described. The catalyst was reusable for up to four reaction sessions.

Graphical abstract

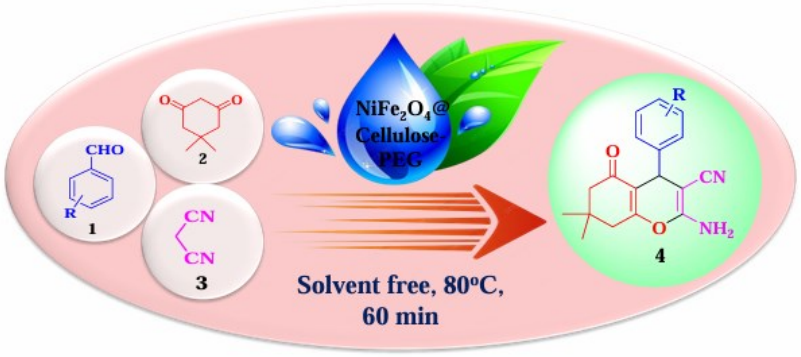

Keywords: $NiFe_2O_4$@Cellulose-PEG, nanocomposite, recyclable catalyst, one-pot multicomponent synthesis, solvent-free, benzopyran.

INTRODUCTION

Research on the synthesis and application of nanomaterials is very intense because of their special physical and chemical characteristics. These materials are significant primarily because of their scientific and technological value. Numerous researchers are drawn to spinel ferrites because of their size, shape, magnetic separation property, reusability, and distinct crystal structure, all of which influence their chemical and physical characteristics. Spinel ferrites and their nanocomposites have grown in popularity in recent years. These materials have several benefits, and their magnetic qualities, which make them easily recovered, allow for recurrent use because of their exceptional catalytic qualities, stability, and reusability. The common formula of spinel ferrite nanoparticles is MFe_2O_4, where M is a transition metal cation [1-4]. Recent years have seen a significant increase in interest in spinel ferrites due to their high chemical and thermal durability, numerous uses in various industries, and superparamagnetic characteristics at the NP scale [5]. Nickel ferrite is one of the most thoroughly investigated spinel ferrites due to its strong magnetic properties and wide variety of uses. Nanosized nickel ferrite possesses favorable properties in addition to the other ferrites that make up a sizable component of magnetic ceramic materials, low-loss materials, soft magnets, and the main parts of high-frequency power transformers. The magnetic characteristics of nickel ferrite are altered by the placement of cations in empty areas [6-8]. This is a crucial element to impress the researchers. Fe^{3+} ions in tetrahedral sites, Fe^{3+} and Ni^{2+} ions in equal amounts at octahedral sites have antiparallel spin magnetic moments, which explains the ferromagnetic nature of this material.

* To whom all correspondence should be sent:
Email: *bhagwatuphade@gmail.com*

One of the most adaptable and technologically relevant soft ferrite materials is nickel ferrite which has low conductivity and thus lowers electrical losses. It has high electrical stability, catalytic activity, and is abundant in nature [9-12].

Biopolymer nanocomposites have attracted a lot of interest because of their unique physicochemical properties and small, inexpensive processing size. Like other natural polysaccharides, cellulose is known to be a harmless, biodegradable, and biocompatible polysaccharide. Because of these qualities, cellulose shows promise as a material for medication delivery and biological applications [13-15].

A well-reported technique for synthesis of physiologically active heterocycles is the multicomponent reaction (MCR). The primary benefits of MCRs over traditional multistep protocols are: high efficiency, low cost, experimental simplicity, avoidance of large amounts of waste, and reduction of labor costs, reaction times, and waste production [16-18]. MCRs are one-pot processes in which at least three or more compounds react together to form the target product without the need for intermediate separation and purification. With the use of green or reusable catalysts and solvent-free conditions, it is possible to achieve ideal synthesis based on the green principles through the development of multicomponent strategies [19, 20].

Tetrahydrobenzo[*b*]pyran derivatives are a significant family of medicines and heterocyclic medications. They show numerous biological and pharmacological activities, including anticancer, diuretic, anticoagulant, spasmolytic, antimalarial, antitumor, antidiabetic, and anti-anaphylactic effects [21-25]. The synthesis of tetrahydrobenzo[*b*]pyran heterocycles has been accomplished using a variety of catalysts such as $Ni(NO_3)_2{\cdot}6H_2O$ [26], Fe_3O_4@xanthan gum [27], SiO_2-Pr-SO_3H [28], $NH_4Al(SO_4)_2{\cdot}12H_2O$ (Alum) [29], $ZnFe_2O_4$@alginic acid [30], nano-SiO_2/DBN [31], DAIL@SiO_2 [32],L-proline [33], DABCO [34], CuONPs [35], K_2CO_3[36], sodium benzoate [37], NH_4OAc [38], PPA-SiO_2 [39], and NiO@HNTs-SO_3H [40], each approach having its own advantages and disadvantages. Here, in continuation of our works [41-46], we investigated the catalytic activity of a novel $NiFe_2O_4$@Cellulose-PEG as a heterogeneous nanocatalyst in the synthesis of tetrahydrobenzo [b]pyran derivatives.

EXPERIMENTAL

The reagents and chemicals used in this work were purchased from Merck and used without further purification. Distilled water was used throughout all work. Using thin-layer chromatography, the progress of the organic reaction was tracked. Melting points of all compounds were ascertained in an open capillary tube. A Bruker Avance NEO 500 MHz spectrometer was used to record the NMR spectra in DMSO with TMS as an internal standard.

Synthesis of $NiFe_2O_4$@Cellulose-PEG

$Fe(NO_3)_3{\cdot}6H_2O$ and $Ni(NO_3)_2{\cdot}6H_2O$ were mixed in 100 ml of distilled water at a molar ratio of 2:1 under stirring for 30 min. Next, 1 g of cellulose powder was added to the solution. 20 ml of 5% NaOH solution was added under constant stirring to adjust pH of the solution between 9 to 10. After 2 h, 1 ml of polyethylene glycol was added to the solution and stirred for more 2 h on a magnetic stirrer. The black precipitate obtained was separated using an external magnet and washed several times with deionized water until neutral pH. The prepared $NiFe_2O_4$@Cellulose-PEG nanocomposite was dried in an oven at 70 °C for 24 h and calcined at 400 °C for 2 h [47].

Synthesis of benzopyran derivatives (4a-k) using $NiFe_2O_4$@Cellulose-PEG

A mixture of substituted benzaldehyde **1a-k** (1 mmol), dimedone **2** (1 mmol), malononitrile **3** (1 mmol), and $NiFe_2O_4$@Cellulose-PEG catalyst (40 mg) was added to a 50 mL round-bottom flask. The combination was heated for the duration shown in Scheme 1 at 80°C in an oil bath without use of solvents. TLC was used to track the reaction progress. After the completion of the reaction, 10 ml of ethanol was added to the reaction mixture to extract the $NiFe_2O_4$@Cellulose-PEG catalyst and the solid product was filtered out. The crude product was recrystallized from ethanol. Melting points and spectroscopic information were used to characterize the products and compare them to those documented in the literature.

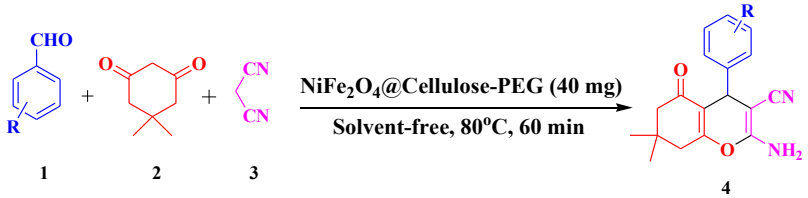

Scheme 1. $NiFe_2O_4$@Cellulose-PEG catalyzed synthesis of tetrahydrobenzo[*b*]pyran derivatives

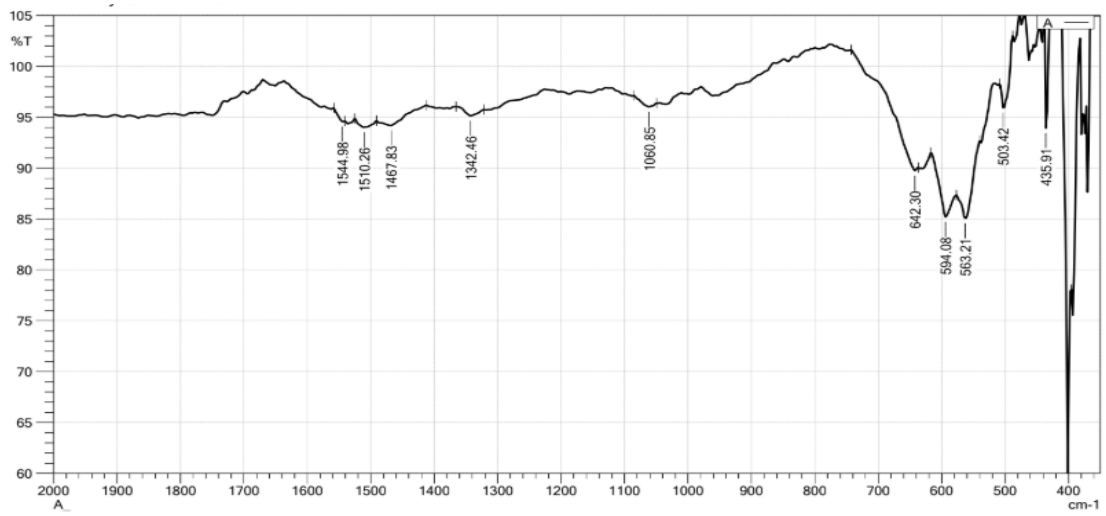

Figure 1. FT-IR spectrum of $NiFe_2O_4$@Cellulose-PEG

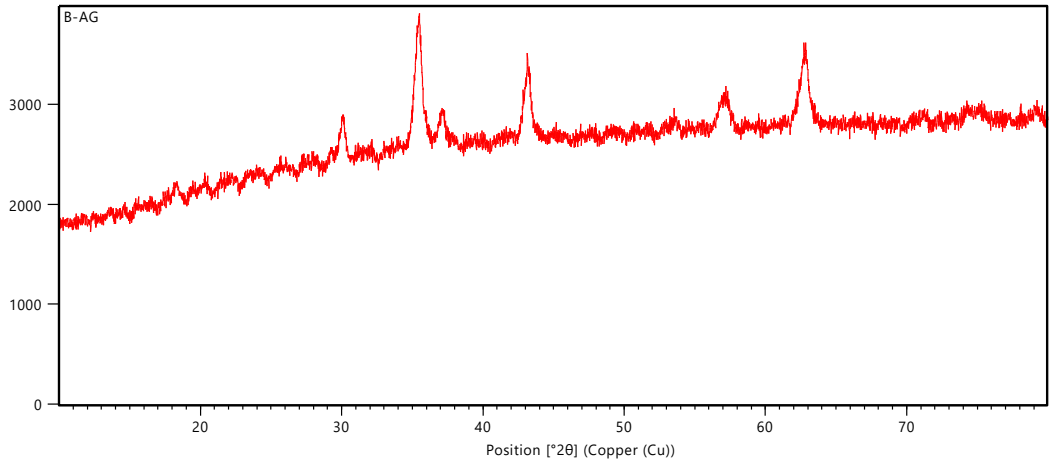

Figure 2. XRD spectrum of $NiFe_2O_4$@Cellulose-PEG

RESULTS AND DISCUSSION

Catalyst characterization

The synthesized nanocatalyst was characterized using a variety of analytical techniques, including Fourier transform infrared (FT-IR) spectroscopy, X-ray powder diffraction (XRD), energy dispersive X-ray spectroscopy (EDX), and field emission scanning electron microscopy (FE-SEM).

FT-IR analysis

The formation of $NiFe_2O_4$@Cellulose-PEG nanocatalyst was confirmed by infrared spectra captured between 400 and 2000 cm^{-1} displayed in Figure 1. The two absorption bands of $NiFe_2O_4$@Cellulose-PEG nanocomposites are visible in the 400-1000 cm^{-1} range. The stretching vibrations of octahedral complexes are associated with the lower absorption band at 435.91 cm^{-1}, while the stretching vibrations of tetrahedral complexes are associated with the higher absorption band at 594.08 cm^{-1}. The absorption band observed at 1510.26 cm^{-1} is due to cellulose doping [48, 49].

XRD analysis

The crystalline structure of the synthesized $NiFe_2O_4$@Cellulose-PEG nanocomposite was confirmed by using the X-ray diffraction (XRD) technique displayed in Figure 2. Diffraction peaks were observed at 2θ values 30.03°, 35.41°, 37.09°, 44.12°, 57.05°, 64.71° (JCPDS Card No. 742081). The sharp and intense peaks indicate a high degree of crystallinity of $NiFe_2O_4$@Cellulose-PEG nanocomposite [50, 51].

EDX analysis

The composition of the synthesized $NiFe_2O_4$@Cellulose-PEG nanocomposite was studied using EDX analysis (see Figure 3). The analysis shows 52.80 wt % and 41.33 at % of iron, 36.88 wt % and 27.34 at % of nickel, 6.44 wt % and 17.52 at % of oxygen, and 3.87 wt % and 14.02 at % of carbon, which supports the formation of $NiFe_2O_4$@Cellulose-PEG nanocomposite.

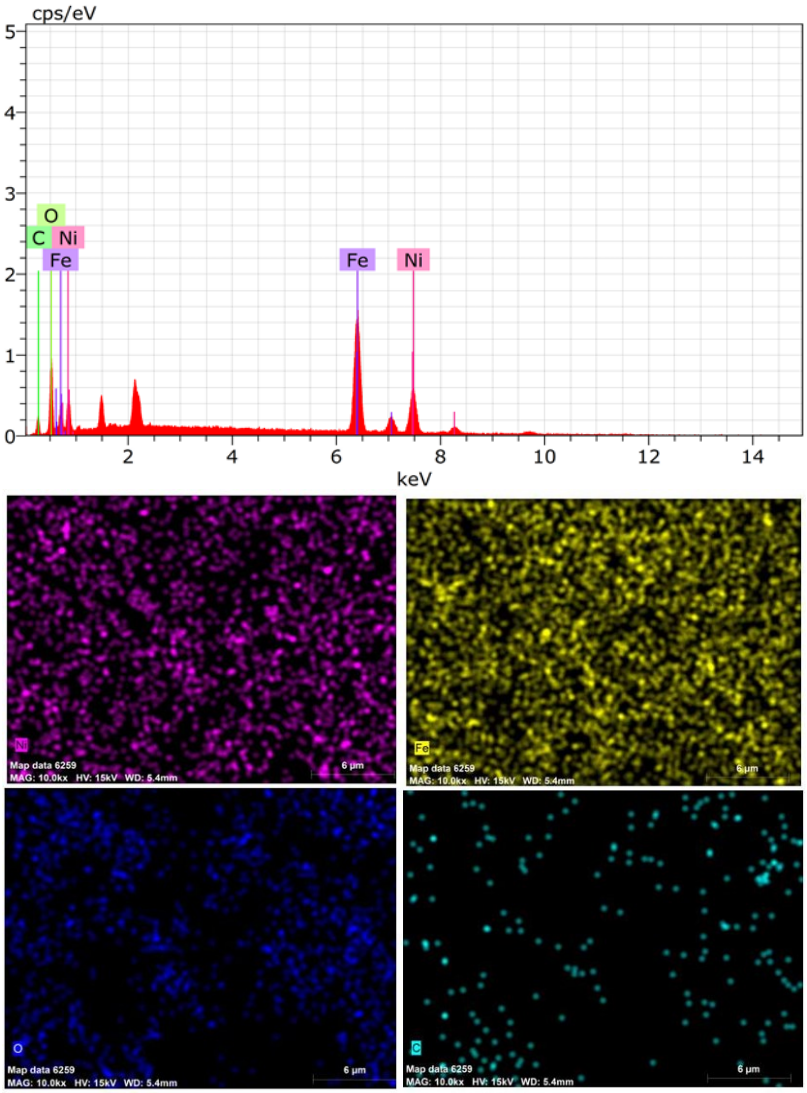

Figure 3. EDX analysis and EDX-MAP images of $NiFe_2O_4$@Cellulose-PEG

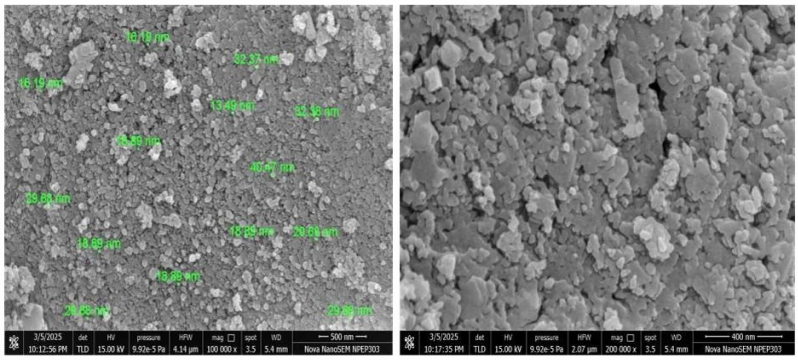

Figure 4. FE-SEM images of $NiFe_2O_4$@Cellulose-PEG

FE-SEM analysis

The surface morphology of the synthesized $NiFe_2O_4$@Cellulose-PEG nanocomposite was investigated using field emission scanning electron microscopy (FE-SEM). The SEM image shown in Figure 4 shows that the particles are uniform and square-shaped, the average particle size is 24.28 nm.

Application of $NiFe_2O_4$@Cellulose-PEG nanocatalyst in the synthesis of benzopyran derivatives

In order to assess the catalytic efficiency of the newly synthesized $NiFe_2O_4$@Cellulose-PEG nanocatalyst, we chose the model reaction between benzaldehyde **1a**, dimedone **2**, and malononitrile **3** for the synthesis of the benzopyran derivative **4a**

under eco-friendly conditions. Several reaction parameters, including temperature and solvents, were optimized (see Table 1). The reaction was conducted under reflux in different solvents such as H_2O, EtOH, and aq. EtOH, which led to insufficient product yield. Subsequently, the model reaction was conducted at various temperatures from 80 °C to 100 °C, without the use of solvents. The optimal temperature for the synthesis of benzopyran derivatives was 80°C without the use of any solvents (Table 1, entry 7). The reaction needed less time to finish and produced a larger product yield.

Table 1. Optimization of reaction conditions for the synthesis of benzopyran derivatives using $NiFe_2O_4$@Cellulose-PEG as a catalyst

Entry	Conditions	Temp. (°C)	Time (min)	Yield (%)[a]
1	H_2O	RT	120	No reaction
2	EtOH	RT	120	No reaction
3	H_2O:EtOH	RT	120	No reaction
4	H_2O	Reflux	60	22
5	EtOH	Reflux	60	36
6	H_2O:EtOH	Reflux	60	43
7	Solvent-free	80	60	94
8	Solvent-free	100	60	94
9	Solvent-free	80	30	91

[a]Reaction conditions: benzaldehyde **1a** (1 mmol), dimedone **2** (1 mmol), malononitrile **3** (1 mmol), and $NiFe_2O_4$@Cellulose-PEG catalyst (40 mg).

Spectral data of some tetrahydrobenzo[b]pyran derivatives

2-amino-5,6,7,8-tetrahydro-7,7-dimethyl-4-(4-nitrophenyl)-5-oxo-4H-chromene-3-carbonitrile (4b). IR (KBr, cm^{-1}): 3315, 3176, 2182, 1671, 1416, 1520, 1352, 1218, ^{1}H NMR (500 MHz, DMSO, δ ppm): 0.98 (*s*, 3H), 1.06 (*s*, 3H), 2.12 (*d*, 1H), 2.24 (*d*, 1H), 2.51 (*s*, 2H), 4.38 (*s*, 1H), 7.16 (*s*, 2H), 7.45 (*d*, 2H), 8.16 (*d*, 2H), ^{13}C NMR (125 MHz, DMSO, δ ppm): 26.8, 28.1, 31.6, 35.5, 39.0, 49.7, 56.9, 111.6, 119.1, 123.5, 128.4, 146.1, 152.1, 158.4, 162.9, 195.5, MS for $C_{18}H_{17}N_3O_4$ (m/z): 340.1[M + H]$^+$.

2-amino-4-(4-chlorophenyl)-5,6,7,8-tetrahydro-7,7-dimethyl-5-oxo-4H-chromene-3-carbonitrile (4e). IR (KBr, cm^{-1}): 3382, 3185, 2188, 1674, 1459, 1216, ^{1}H NMR (500 MHz, DMSO, δ ppm): 0.95 (*s*, 3H); 1.03 (*s*, 3H), 2.08 (*d*, 1H), 2.22 (*d*, 1H), 2.48 (*s*, 2H), 4.22 (*s*, 1H), 7.05 (*s*, 2H), 7.18 (*d*, 2H), 7.33 (*d*, 2H), ^{13}C NMR (125 MHz, DMSO, δ ppm): 26.7; 28.3, 31.6, 35.6, 39.1, 49.8, 57.8, 112.6, 119.4, 126.2, 129.0, 131.1, 144.6, 158.4, 162.7, 195.5, MS for $C_{18}H_{17}ClN_2O_2$ (m/z): 329.1 [M + H]$^+$.

Further, the effect of catalyst loading on the model reaction was investigated. As shown in Table 2, the maximum yield was obtained with 40 mg of the catalyst (entry 4). The yield and reaction rate were not enhanced by additional catalyst loading (entry 5). A benzopyran derivative was produced with 94% yield using 40 mg of the catalyst at 80°C without the use of solvents.

Table 2. Effect of catalyst loading on the synthesis of benzopyran derivatives under solvent-free conditions at 80°C

Entry	Amount of catalyst (mg)	Reaction time (min)	Yield (%)[a]
1	10	60	69
2	20	60	83
3	30	60	91
4	**40**	**60**	**94**
5	50	60	94
6	60	60	94

[a]Reaction conditions: benzaldehyde **1a** (1 mmol), dimedone **2** (1 mmol), malononitrile **3** (1 mmol), and $NiFe_2O_4$@Cellulose-PEG as a catalyst.

After determining the optimal reaction conditions, we investigated the scope of the suggested methodology by applying several substituted benzaldehydes **1a-k** with dimedone and malononitrile at 80°C under solvent-free conditions in the presence of $NiFe_2O_4$@Cellulose-PEG nanocatalyst. As shown in Table 3, whether the aromatic aldehyde had an electron-donating or electron-withdrawing substituent, the reaction was equally simple and produced the intended benzopyran derivatives in high yields. Physical characteristics were used to describe the products.

The catalytic activity of the $NiFe_2O_4$@Cellulose-PEG nanocatalyst was compared to that of a few other documented catalysts, as shown in Table 4. It can be concluded that the $NiFe_2O_4$@Cellulose-PEG nanocatalyst has superior catalytic efficiency, making it the most efficient catalyst which gives high product yields in a noticeably shorter duration.

Table 3. $NiFe_2O_4$@Cellulose-PEG catalyzed one-pot synthesis of benzopyran derivatives under solvent-free conditions at 80°C

Entry	Aldehyde	Product	Time (min)	Yield (%)[a]	M. P. (°C)	
					Observed	Reported
4a		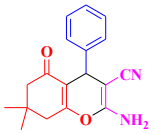	60	94	226-228	226-228
4b	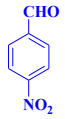	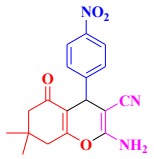	50	94	182-184	186-188
4c		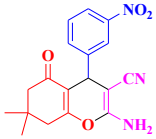	60	91	216-218	212-214
4d	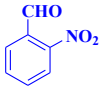	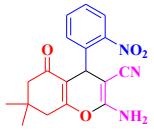	60	90	228-230	224-226
4e	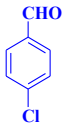	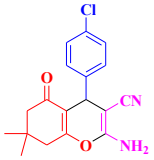	50	94	200-202	198-200
4f		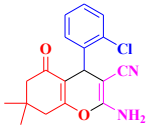	60	88	208-210	210-212
4g	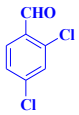	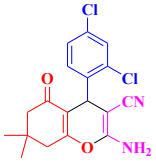	50	90	122-124	118-120
4h	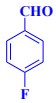	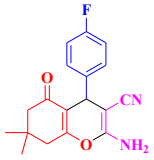	50	93	174-176	178-180
4i	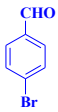	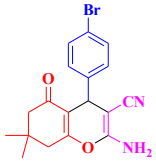	55	92	198-200	202-204
4j	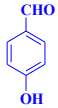	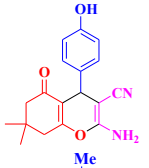	60	90	204-206	208-210
4k	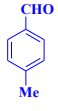	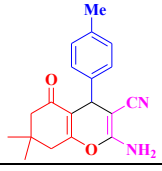	65	92	222-224	218-220

Table 4: Comparison of $NiFe_2O_4$@Cellulose-PEG catalyst with reported catalysts for the synthesis of benzopyran derivatives

Entry	Catalyst	Reaction conditions	Time (min)	Yield (%)	Reference
1	SiO_2-Pr-SO_3H	H_2O/Reflux	8	88	[28]
2	$NH_4Al(SO_4)_2$	EtOH/80°C	120	92	[29]
3	$ZnFe_2O_4$@alginic acid	EtOH/RT	10	93	[30]
4	nano-SiO_2/DBN	H_2O: EtOH/60°C	15	93	[31]
5	DAIL@SiO_2	SF/100°C	120	86	[32]
6	L-Proline	EtOH/Reflux	30	92	[33]
7	DABCO	H_2O/Reflux	120	89	[34]
8	$NiFe_2O_4$@Cellulose-PEG	SF/80°C	60	94	This work

Catalyst reusability

The model reaction between benzaldehyde **1a** (1 mmol), dimedone **2** (1 mmol), and malononitrile **3** (1 mmol) in the presence of $NiFe_2O_4$@Cellulose-PEG nanocatalyst at optimal reaction conditions was examined to determine the recyclability of the nanocatalyst. Following a successful reaction, hot ethanol was added to the reaction mixture, the nanocatalyst was filtered out, thoroughly washed with distilled water, and then dried for 1 h at 100 °C. The recovered catalyst worked properly up to four cycles (Figure 5).

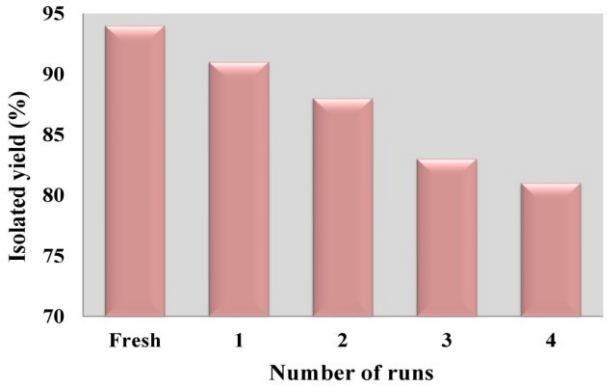

Figure 5. Reusability of $NiFe_2O_4$@Cellulose-PEG nanocatalyst

CONCLUSION

The current study successfully used a simple, economical, and effective method for obtaining $NiFe_2O_4$@Cellulose-PEG nanocatalyst in a solvent-free, one-pot multicomponent reaction of various aromatic aldehydes, dimedone, and malononitrile at 80°C. Characteristics such as straightforward reactions, non-toxic catalysts, straightforward purification, mild reaction conditions, and high product yield are the key components of this green-chemical methodology. The catalyst was recycled and reused without substantially lowering the catalytic activity for four runs.

Disclosure statement: *The authors declare that they have no relevant or material financial interests that relate to the research described in this paper.*

Declaration of funding: *No funding was received.*

Conflict of interest: *The authors declare no conflict of interest, financial or otherwise.*

Acknowledgement: *The authors are thankful to the Management and Principal, P. V. P. College, Pravaranagar for providing laboratory facilities and constant encouragement during the work. The authors are also thankful to the SAIF, Panjab University, Chandigarh, for the spectral analysis.*

REFERENCES

1. S.J. Salih, W.M. Mahmood, *Heliyon*, **9**, 6 (2023).
2. M. Amiri, M. Salavati-Niasari, A. Akbari, *Adv. Colloid Interface Sci*., **265**, 29 (2019).
3. A. Hajalilou, S.A. Mazlan, *Appl. Phys. A*, **122**, 680 (2016).
4. A. Soufi, H. Hajjaoui, W. Boumya, A. Elmouwahidi, E. Baillon-Garcia, M. Abdennouri, N. Barka, *J. Environ. Manage*., **367**, 121971 (2024).
5. A.Q. Malik, H. Singh, A. Kumar, R. Aepuru, D. Kumar, T. Gani Mir, Q. Ain, A.A. Bhat, *ES Energy and Environment*, **19**, 744 (2023).
6. Z.K. Heiba, M.B. Mohamed, L. Arda, N. Dogan, *J. Magn. Magn. Mat*., **391**, 195 (2015).
7. R. Choubey, D. Das, S. Mukherjee, *J. Alloys Compd*., **668**. 33 (2016).
8. D.M. Wu, X.P. Liu, P.Z. Gao, L.T. He, J.W. Li, *Ceram. Int*., **48**, 11228, (2022).
9. U. Ahmad, M. Afzia, F. Shah, B. Ismail, A. Rahim, R.A. Khan, *Mater. Sci. Semicond. Process*., **148**, 106830 (2022).
10. N. Gupta, P. Jain, R. Rana, S. Shrivastava, *Mater. Today Proc*., **4**, 342 (2017).
11. S.P. Dalawai, S. Kumar, M.A. Aly, M.Z. Khan, R. Xing, P.N. Vasambekar, S. Liu, *J. Mater. Sci.: Mater. Electron*., **30**, 7752 (2019).
12. R.S. Rajenimbalkar, V.J. Deshmukh, K.K. Patankar, S.B. Somvanshi, *Sci. Rep*., **14**, 29547 (2024).
13. V. Gopinath, S. Saravanan, A.R. Al-Maleki, M. Ramesh, J. Vadivelu, *Biomed. Pharmacother*., **107**, 96 (2018).
14. I. Benalaya, G. Alves, J. Lopes, L.R. Silva, *Int. J. Mol. Sci*.,**25**, 1322 (2024).

15. S. Sharma, M. Bhende, *Polym. Bull*., **81**, 12383 (2024).
16. R.C. Cioc, E. Ruijter, R.V. Orru, *Green Chem*., **16**, 2958 (2014).
17. H.A. Younus, M. Al-Rashida, A. Hameed, M. Uroos, U. Salar, S. Rana, K.M. Khan, *Expert Opin. Ther. Pat.,* **31**, 267 (2021).
18. B.S. Vachan, M. Karuppasamy, P. Vinoth, S.V. Kumar, S. Perumal, V. Sridharan, J.C. Menendez, *Adv. Synth. Catal*., **362**, 87 (2020).
19. M.B. Gawande, V.D. Bonifacio, R. Luque, P.S. Branco, R.S. Varma, *ChemSusChem*,**7**, 24 (2014).
20. A. Sarkar, S. Santra, S.K. Kundu, A. Hajra, G.V. Zyryanov, O.N. Chupakhin, V.N. Charushin, A. Majee, *Green Chemistry*, **18**, 4475 (2016).
21. M.A. Bodaghifard, M. Solimannejad, S. Asadbegi, S. Dolatabadi Farahani, *Res. Chem. Intermed*., **42**, 1165 (2016).
22. M. Abaszadeh, M. Seifi, S.Y. Ebrahimipour, *Bull. Chem. Soc. Ethiop*., **30**, 253 (2016).
23. G.M. Ziarani, A. Abbasi, A. Badiei, Z. Aslani, *J. Chem*., **8**, 293 (2011).
24. S. Mostafa Habibi-Khorassani, M. Shahraki, E. Mollashahi, S. Shadfar Pourpanah, S. Keshavarz Majdabadi, *Comb. Chem. High Throughput Screen*., **19**, 865 (2016).
25. H.R. Saadati-Moshtaghin, F.M. Zonoz, *Mater. Chem. Phys*., **199**, 159 (2017).
26. B. Boumoud, A.A. Yahiaoui, T. Boumoud, A. Debache, *J. Chem. Pharm. Res*., **4**, 795 (2012).
27. M.S. Esmaeili, M.R. Khodabakhshi, A. Maleki, Z. Varzi, *Polycycl. Aromat. Compd*., **41**, 1953 (2021).
28. G.M. Ziarani, A. Abbasi, A. Badiei, Z. Aslani, *J. Chem*., **8**, 293 (2011).
29. A.A. Mohammadi, M.R. Asghariganjeh, A. Hadadzahmatkesh, *Arab. J. Chem*., **10**, S2213 (2017).
30. A. Maleki, Z. Varzi, F. Hassanzadeh-Afruzi, *Polyhedron*, **171**, 193 (2019).
31. M. Mehravar, B.B. Mirjalili, E. Babaei, A. Bamoniri, *BMC Chem*., **15**, 34 (2021).
32. Q. Zhang, H. Wei, J. Li, X. Zhao, J. Luo, *Heterocycl. Commun*., **23**, 411 (2017).
33. P. Kate, V. Pandit, V. Jawale, M. Bachute, *J. Chem. Sci*., **134**, 4 (2022).
34. D. Tahmassebi, J.A. Bryson, S.I. Binz, *Synth. Commun*., **41**, 2701 (2011).
35. A. Mulik, P. Hegade, S. Mulik, M. Deshmukh, *Res. Chem. Intermed*., **45**, 5641 (2019).
36. Z.K. Jaberi, B. Pooladian, *Sci. World J*., 208796 (2012).
37. H. Ostadzadeh, H. Kiyani, *Polycycl. Aromat. Compd*., **43**, 9318 (2023).
38. A.M. Zonouz, S. Okhravi, D. Moghani, *Monatsh. Chem*., **147**, 1819 (2016).
39. A. Davoodnia, S. Allameh, S. Fazli, N. Tavakoli-Hoseini, *Chem. Pap*., **65**, 714 (2011).
40. V. Vikhe, A. Kshirsagar, B. Uphade, A. Gadhave, *Res. Chem. Intermed*., **50**, 4199 (2024).
41. V. Vikhe, D. Aute, V. Kadnor, G. Shirole, B. Uphade, A. Gadhave, *Polycycl. Aromat. Compd*., **45**, 322 (2025).
42. A.K. Mhaske, A.G. Gadhave, A.G. Dholi, B.K. Uphade, *J. Inorg. Organomet. Polym. Mater*., **34**, 999 (2024).
43. P.D. Ladkat, P.K. Gadekar, V.M. Khedkar, B.K. Uphade, A.G. Gadhave, *ChemistrySelect.*, **10**, e202404836 (2025).
44. A.R. Parhad, D.S. Aute, A.G. Gadhave, B.K. Uphade, *Polycycl. Aromat. Compd*., **44**, 5261 (2024).
45. A.K. Mhaske, D.V. Vikhe, A.G. Gadhave, B.K. Uphade, *Polycycl. Aromat. Compd*., **45**, 490 (2025).
46. V.V. Vikhe, A.K. Mhaske, V.K. Vikhe, B.K. Uphade, A.G. Gadhave, *Catal. Surv. Asia*, **29**, 249 (2025).
47. P. Sivakumar, R. Ramesh, A. Ramanand, S. Ponnusamy, C. Muthamizhchelvan, *Mater. Lett*., **65**, 483 (2011).
48. Z. Li, M. Ye, A. Han, H. Du, *J. Mater. Sci.: Mater. Electron*., **27**, 1031 (2016).
49. S. Nam, A.D. French, B.D. Condon, M. Concha, *Carbohydr.Polym*., **135**, 1 (2016).
50. W.E. Pottker, R. Ono, M.A. Cobos, A. Hernando, J.F. Araujo, A.C. Bruno, S.A. Lourenço, E. Longo, F.A. La Porta, *Ceram. Int*., **44**, 17290 (2018).
51. M. Abushad, M. Arshad, S. Naseem, H. Ahmed, A. Ansari, V.K. Chakradhary, S. Husain, W. Khan, *J. Mol. Struct*., **1253**, 132205 (2022).